Journal of Thermal Analysis, Vol. 50 (1997) 409-423

CURE KINETICS OF AN EPOXY SYSTEM CONTAINING TETRAGLYCIDYL-4,4′-DIAMINODIPHENYLMETHANE (TGDDM) AND A MULTIFUNCTIONAL NOVOLAC GLYCIDYL ETHER CURED WITH 4,4′-DIAMINODIPHENYLSULFONE (DDS)

L. Barral, J. Cano, J. López, P. Nogueira, M. J. Abad and C. Ramírez

Departamento de Física. Universidad de A Coruna. E. U. P. Ferrol. Cra. Aneiros s/n. 15405 Ferrol, Spain

(Received May 15, 1996; in revised form December 6, 1996)

Abstract

Differential scanning calorimetry (DSC) was applied to study the cure kinetics of an epoxy system containing both tetraglycidyl 4,4′-diaminodiphenylmethane (TGDDM) and a multifunctional Novolac glycidyl ether resin, cured with 4,4′-diaminodiphenylsulfone (DDS). The experimental data were analyzed in terms of a mechanistic model proposed by Cole, which includes the etherification reaction. The kinetics can be completely described in terms of three rate constants, which obey the Arrhenius relationship. This model gives a good description of the cure kinetics up to the onset of vitrification. The effect of diffusion control was incorporated to describe the cure in the later stages. By combining the model and a diffusion factor, it was possible to predict the cure kinetics over the whole range of conversion, including an analysis of the evolution of different chemical species during the curing process. Good agreement with the experimental DSC data was achieved with this mechanistic model over the whole range of cure when the etherification reaction was assumed to be of first order with respect to the concentrations of epoxide groups, hydroxy groups, and the tertiary amine groups formed in the epoxide amine reaction.

Keywords: cure kinetics, DSC, etherification, TGDDM epoxy

Introduction

Tetraglycidyl-4-4′-diaminodiphenylmethane (TGDDM) epoxy is an ideal material for many important usages; it is especially used as a matrix for fiber-reinforced composites. There are some commercial epoxy formulations of great significance in the manufacture of high-performance composites that utilize more than one epoxy to aid in processing or to improve properties. A great num-

0368–4466/97/ $ 5.00

John Wiley & Sons Limited
Chichester

ber of them are made of two epoxies, TGDDM and a Novolac resin, which are cured with 4,4′-diaminodiphenylsufone (DDS).

TGDDM/DDS epoxy systems have been extensively studied [1–4], but there are only a few papers on TGDDM/Novolac/DDS systems [5–7]. In the present study, the cure kinetics of a TGDDM/Novolac/DDS epoxy system was investigated by differential scanning calorimetry (DSC) under isothermal conditions. The objective of this work was to provide an accurate description of the cure kinetics not only in the early stages of the cure reaction, but also in the later stages, where the vitrification effect is dominant and the reaction is controlled by diffusion instead of chemical kinetics. To model the polymerization reaction kinetics of this system, a mechanistic approach used by Cole [8], which includes the etherification reaction, was developed.

Although epoxy amine reactions are complicated, depending on the reaction conditions, it is generally accepted that there are two important amine addition reactions [9, 10]. The first occurs between an epoxide ring (E) and a primary amine group (A_1) to produce a link containing a secondary amine group (A_2) and a hydroxy group (OH). The secondary amine group formed in this reaction can react further to give a tertiary amine group (A_3) and a new OH group. The third type of reaction that can occur is etherification, which is a reaction between an epoxide and the OH group to form an ether link and a new OH group [11]. The etherification reaction is slower than the epoxide amine reaction and becomes important only when the cure is performed at high temperatures or when there is an excess of epoxy with respect to amine [12].

A resin system can be regarded as an association of epoxide groups, amine groups, OH groups, ether groups and catalysts. Following Cole, we have assumed that the unreacted resin contains only epoxide, primary and tertiary amine, OH and catalyst (other than OH) groups (X), and the proposed reaction scheme is:

$$E + A_1\,(+\mathrm{OH}) \xrightarrow{k_1} A_2 + \mathrm{OH}\,(+\mathrm{OH})$$

$$E + A_1\,(+X) \xrightarrow{k_1'} A_2 + \mathrm{OH}\,(+X)$$

$$E + A_2\,(+\mathrm{OH}) \xrightarrow{k_2} A_3 + \mathrm{OH}\,(+\mathrm{OH})$$

$$E + A_2\,(+X) \xrightarrow{k_2'} A_3 + \mathrm{OH}\,(+X)$$

$$E + m\mathrm{OH} + nA_3 \xrightarrow{k_3} \mathrm{ether} + m\mathrm{OH} + nA_3$$

The first four equations are equivalent to those used by Horie [13]. The fifth represents the etherification reaction, with m representing the number of OH groups involved (as either reactant or catalyst) and n the number of A_3 groups (as catalyst).

The kinetic equations for the above reaction scheme can be solved to give the following two equations in terms of the variables α and β. The first is the epoxide conversion and the second is a measure of the number of OH groups produced by the reaction:

$$\alpha = B\beta + \frac{K_3}{K_1 + BK_2}\left(C_1\beta + C_2\beta^2 + C_3\ln(1 + R^{-1}\beta) + C_4\ln(1 - \beta)\right) \quad (1)$$

$$\frac{d\alpha}{dt} = \left(B(K_1 + BK_2\beta)(1 - \beta) + K_3(Y + \beta)^m(Z + \beta^2)^n\right)(1 - \alpha) \quad (2)$$

where all parameters of these equations have been defined previously [7, 8]. K_1 is the rate constant for the epoxide amine reaction catalyzed by groups initially present in the resin (including OH), K_2 is the rate constant for the same reaction catalyzed by OH groups formed in the reaction, and K_3 is the rate constant for the etherification reaction. The coefficients C_i depend on the values of m and n; the various pairs of values m and n represent different possibilities for the etherification reaction mechanism, B is the amine to epoxide ratio in the unreacted resin, Y is a measure of the OH content in the unreacted resin, Z, is a measure of the tertiary amine content in the unreacted resin, and $R=K_1/BK_2$.

If the variables α and β are used to model the cure, it is possible to follow quantitatively the two reaction paths, epoxy amine and etherification. The relative importance of these will vary, depending on the temperature. Once the three rate constants are known, the cure can be completely described, including the evolution of the different chemical species as a function of the degree of cure.

Experimental

The epoxy resin system studied was a mixture of three components. The main one is tetraglycidyl- 4,4′-diaminodiphenylmethane (TGDDM) (Ciba-Geigy MY 720), the second component is a multifunctional Novolac glycidyl ether resin (Ciba-Geigy EPN 1138) and the third is an aromatic amine hardener, 4,4′-diaminodiphenylsulfone (DDS), available from Fluka Chemie.

All these components were used as received. The composition of the mixture was 43.3% of TGDDM, 35.7% of EPN and 21.0% of DDS, yielding an amine-epoxide ratio of B=0.64, based on the epoxide equivalent weights determined in our laboratory by hydrochlorination [14]. The values obtained for the weight per epoxy equivalent for TGDDM and EPN, respectively, were 130 and 180 g/eq. The hardener has a molecular weight of 248.31 and a purity >96% according to the supplier. The material was prepared by mixing the components in an oven at 120°C and stirring continuously until a homogeneous mixture was achieved.

DSC under dynamic and isothermal conditions was used to study the cure kinetics of this system. DSC measurements were made with a Perkin Elmer DSC-7

calorimeter supported by a Perkin Elmer Computer for data acquisition. The DSC was calibrated with indium and zinc standards. All experiments were conducted under a nitrogen flow of 40 ml min^{-1}.

For dynamic experiments, heating rates of 2.5, 5, 7.5 and 10°C min^{-1} were investigated from 25 to 300°C. In isothermal experiments, the DSC was stabilized to 25°C. Samples of about 15 mg were enclosed in aluminum capsules, introduced into the DSC cell, and then heated at high rate to the experimental temperature, ranging from 210 to 240°C. The total area under the exotherm curve, based on the extrapolated baseline at the end of the reaction, was used to calculate the isothermal heat of cure.

Results and discussion

If the cure reaction is the only thermal event, then the reaction rate $d\alpha/dt$ is equal to the heat flow, dH/dt, divided by the overall heat of reaction ΔH_o:

$$\frac{d\alpha}{dt} = \frac{dH/dt}{\Delta H_o} \tag{3}$$

Figure 1 shows the DSC dynamic scans at different heating rates. The overall heat evolved in the reaction was determined as the average reaction heat calculated in each DSC curve. The corresponding value found for the TGDDM/Novolac/DDS system was ΔH_o=642.1 J g^{-1}.

Isothermal DSC curves are shown in Fig. 2, plotted as $d\alpha/dt$ *vs.* time. From the experimental data, it is possible to construct a curve of $d\alpha/dt$ *vs.* α for each curing temperature and to test these data with the model proposed by Cole. This model describes different possibilities for the etherification reaction mecha-

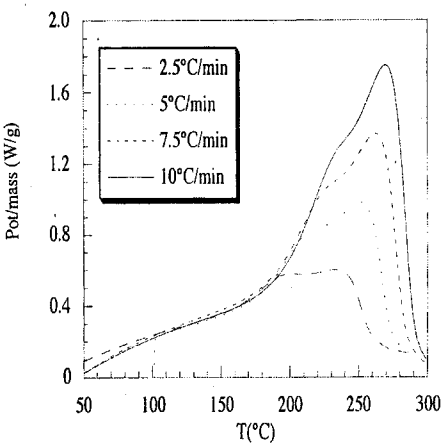

Fig. 1 DSC dynamic runs at different heating rates

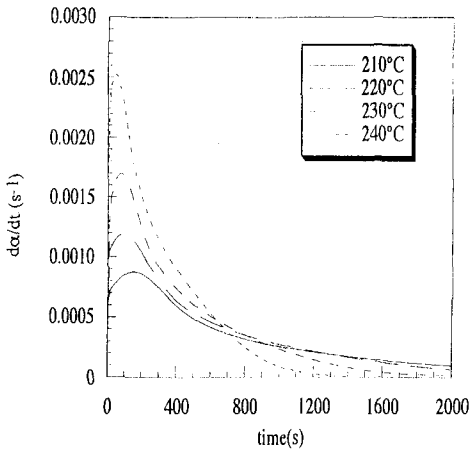

Fig. 2 Reaction rate, $d\alpha/dt$, *vs.* time curves for different curing temperatures

nism. Regardless of the particular mechanism, this model includes three rate constants, that must be determined to obtain the best fit of the experimental data for $d\alpha/dt$ as a function of α. To determine the constants, an iterative procedure was used. After initial estimates for K_1, K_2 and K_3 had been chosen, for each experimental value of α the corresponding value of β was calculated by numerical solution of Eq. (1). The values of α and β were then used in Eq. (2) to calculate $d\alpha/dt$. The coefficient Y was assumed to be negligible.

Initial estimations for K_1 and K_2 were chosen from the fit of the experimental data with the simplified Horie equation [13]:

$$\frac{d\alpha}{dt} = (K_1 + K_2\alpha)(1 - \alpha)(B - \alpha) \tag{4}$$

Figure 3 shows plots of the reduced rate function $F_1(\alpha)=(1-\alpha)^{-1}(B-\alpha)^{-1}$ $(d\alpha/dt)$ *vs.* α for the different temperatures. Except for the first few points, linear behavior is observed up to α about 0.2. When $\alpha>0.3$, there is a significant deviation, which is attributed to the lack of validity of the model proposed by Horie in this region, where the etherification reaction becomes significant.

The initial estimation of K_3 was made from the fit of the data with the extension of the Horie model used by Lee *et al.* [15]. In this approach, the reaction is separated in to two distinct stages. For $\alpha<0.3$, only the epoxide amine reaction need be considered, and Eq. (4) is used. When this reaction has been completed, the etherification reaction takes over, and the etherification is assumed to be of first order with respect to the epoxide concentration, when it can be described by the equation

$$\frac{d\alpha}{dt} = K_3(1 - \alpha) \tag{5}$$

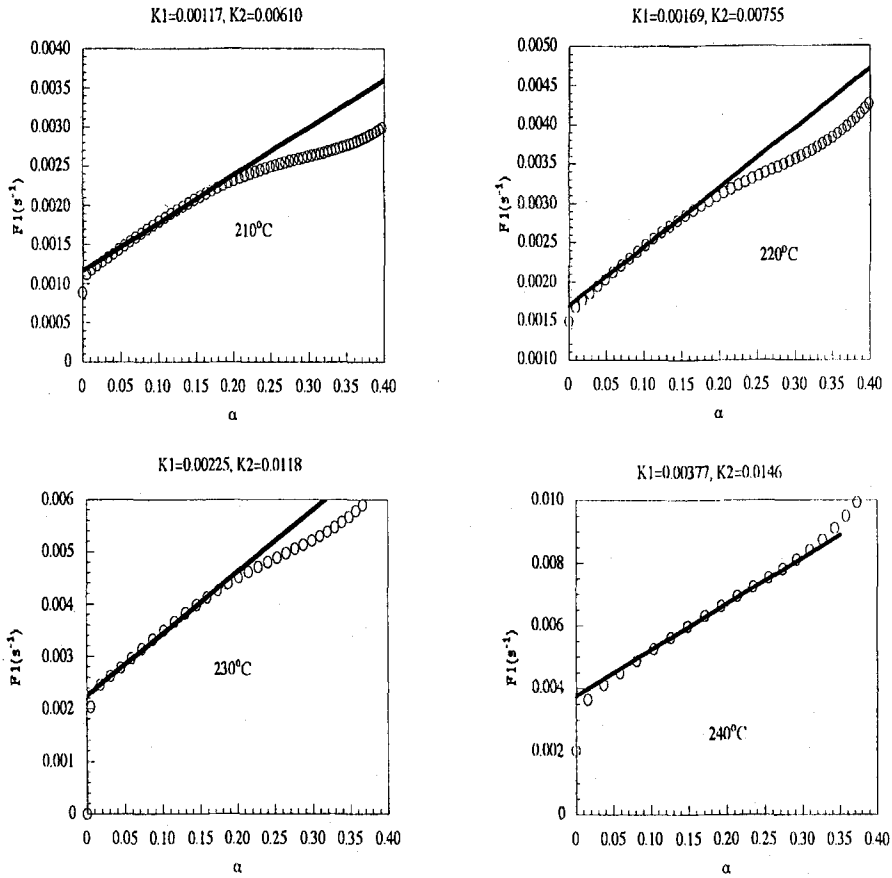

Fig. 3 Plots of $F_1(\alpha)=(1-\alpha)^{-1}(B-\alpha)^{-1}(d\alpha/dt)$ *vs.* conversion at different curing temperatures

In this case, the reduced function $F_2(\alpha)=(1-\alpha)^{-1}d\alpha/dt$ should be constant and equal to K_3. The function F_2 was plotted *vs.* α, as shown in Fig. 4. It can be seen that F_2 rises to a maximum value at around $\alpha=0.2$, and gradually decreases until α reaches about 0.7 or 0.8, where there is an abrupt drop and the reaction rate falls to zero. This is believed to be due to vitrification of the system and the onset of diffusion control. It can be seen too that, as the temperature is elevated, F_2 becomes more constant, i.e. the etherification reaction is more effective.

The best fit of our data corresponded to the case where the etherification reaction was taken as of first order with respect to epoxide groups (E), OH groups and the tertiary amine groups formed in the reaction (A_3), so this mechanism was used to analyze the data and determine the three rate constants for all experiments.

A comparison of typical experimental DSC data and predictions of the model proposed by Cole is shown in Fig. 5. A reasonably good fit between the experimental data and the predictions of the model is achieved. However, the model

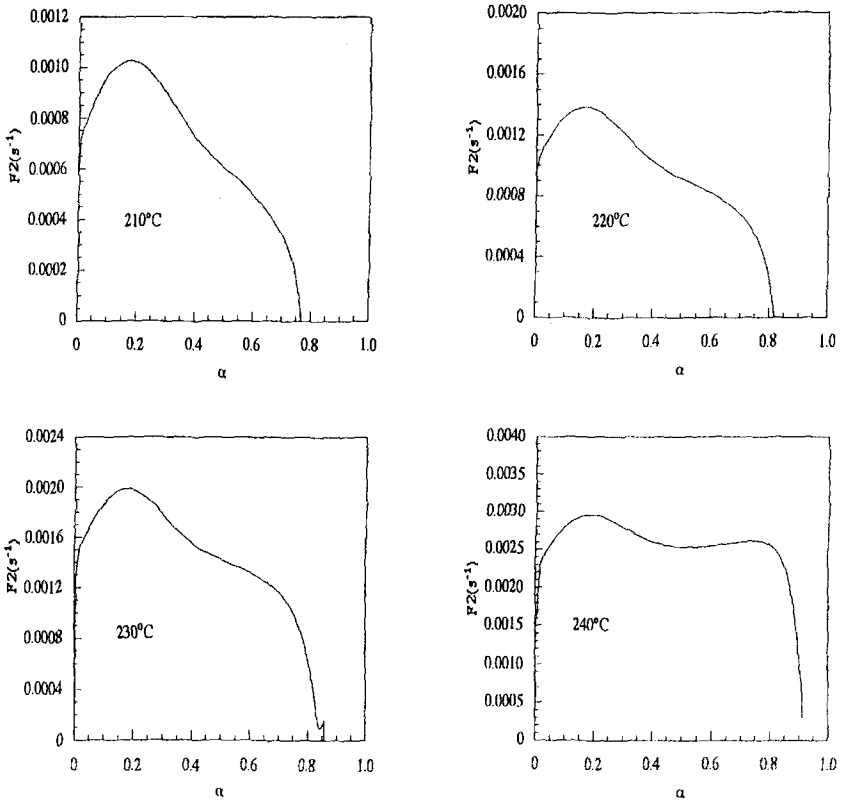

Fig. 4 Plots of $F_2(\alpha)=(1-\alpha)^{-1}(d\alpha/dt)$ *vs.* conversion at different curing temperatures

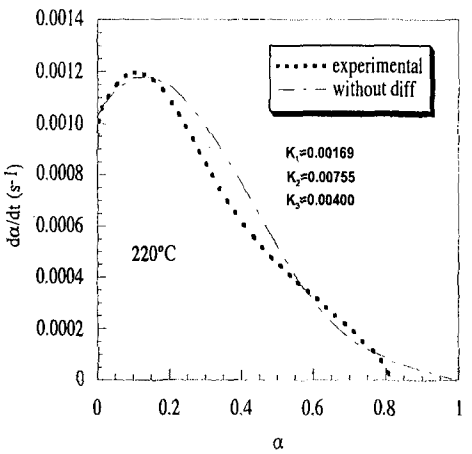

Fig. 5 Comparison of experimental data with the proposed model: reaction rate, $d\alpha/dt$, *vs.* conversion, α

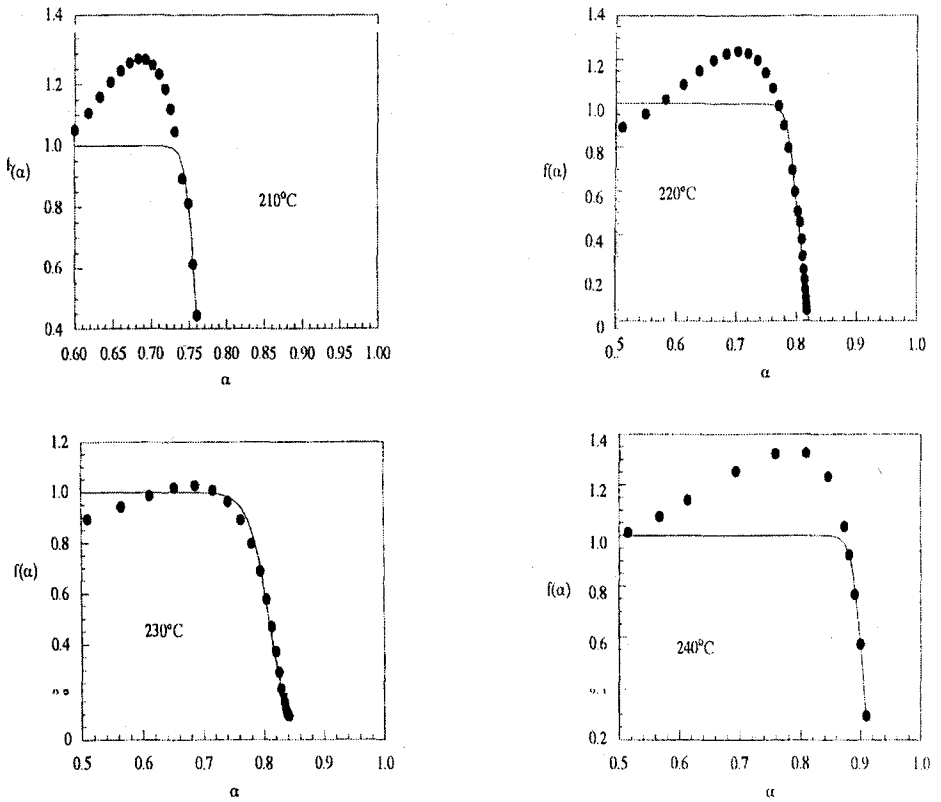

Fig. 6 Diffusion factor, $f(\alpha)$, *vs.* conversion, α, and the regression fit obtained with Eq. (6)

predicts higher conversions and reaction rates for the later stages of the cure reaction. The deviations observed are attributed to the reaction becoming diffusion-controlled at the onset of vitrification. On the other hand, the deviations observed for α between 0.2 and 0.5 will be commented on below.

To consider the diffusion effect, we used a semiempirical relationship, based on free volume considerations, proposed by Chern and Poehlein [16]. In this relationship, a diffusion factor, $f(\alpha)$, has been introduced and defined as the ratio K_e/K_c, where K_c is the rate constant for chemical kinetics and K_e is the overall effective rate constant; according to Rabinowich [17], K_e includes the effects of both chemical kinetics and diffusion. This diffusion factor is given by

$$f(\alpha) = \frac{K_e}{K_c} = \frac{1}{1 + \exp[C(\alpha - \alpha_c)]} \tag{6}$$

where C is a constant and α_c is the critical value of conversion at which the effect of diffusion becomes important. When $\alpha << \alpha_c$, $f(\alpha)$ approximates to unity, the

reaction is kinetically controlled, and the effect of diffusion is negligible. As α approaches α_c, $f(\alpha)$ begins to decrease, and it approaches zero, as the reaction effectively stops. Equation (6) corresponds to a rather abrupt onset of diffusion control at $\alpha=\alpha_c$; however, the onset is more gradual, and there is a region where both chemical and diffusion factors are controlling. The factor $f(\alpha)$ was obtained as the ratio of the experimental reaction rate values to those predicted on the basis of the chemical kinetic model. Figure 6 shows plots of $f(\alpha)$ against conversion at different curing temperatures, and also the regression fits obtained with Eq. (6). Although the fits do not seem very good, the zone of interest is the last part of the plots, where the diffusional effect is pronounced.

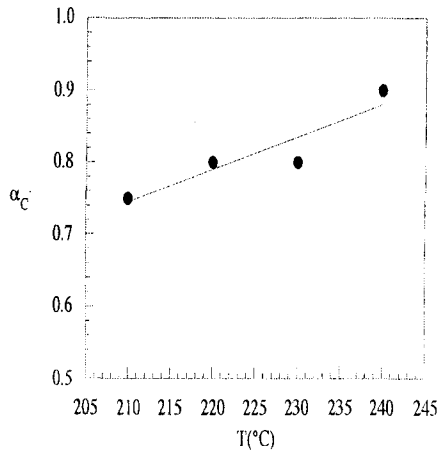

Fig. 7 Values of critical conversion, α_c, *vs.* curing temperatures

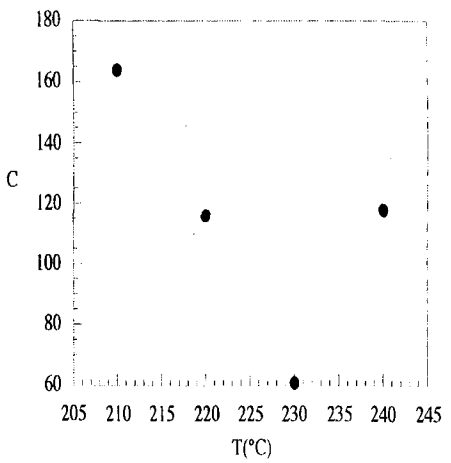

Fig. 8 Values of parameter *C vs.* curing temperatures

Table 1 Arrhenius parameters for the proposed model

Rate constant/s^{-1}	$\ln A$	$\frac{E_a}{R}$/K	E_a/kJ mol^{-1}
K_1	13.46	9801	81.45
K_2	9.61	7090	58.92
K_3	29.82	18546	154.12

Values of α_c and C *vs.* curing temperatures, obtained by fitting the $f(\alpha)$ *vs.* α data to Eq. (6), are shown in Figs 7 and 8. Linear behavior with temperature is observed for α_c, but for the coefficient C no discernible trend is observed, in accord with findings from other studies on epoxy amine systems [18, 19].

Figure 9 depicts the results for each curing temperature when the experimental values of $d\alpha/dt$ are compared with those calculated via the model with the diffusion factor included. Good agreement was found over the whole curing tem-

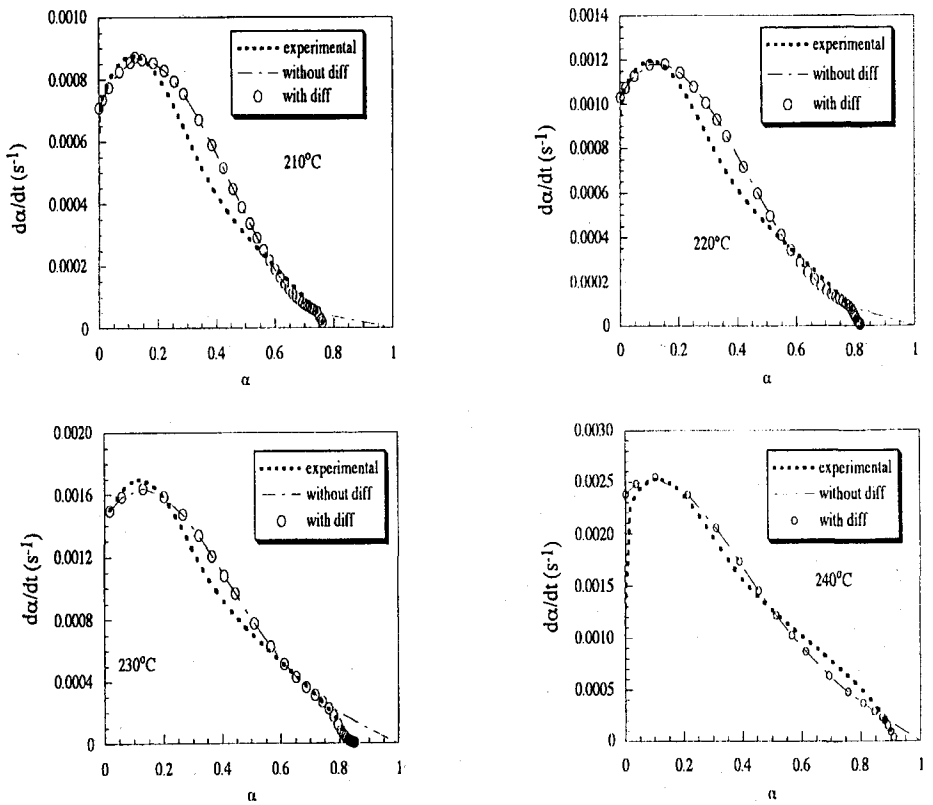

Fig. 9 Comparisons of experimental data with model prediction: reaction rate, $d\alpha/dt$, *vs.* conversion, α, at different temperatures

perature range, except for the α interval between 0.2 and 0.5 for curing temperatures of 210 and 220°C.

The three rate constants obey the Arrhenius relationship $K_i=A_i\exp(-Ea_i/RT)$. The Arrhenius plots of $\ln K_i$ *vs.* $1/T$ led to the parameters given in Table 1. The activation energies for the *X*-catalyzed and OH-catalyzed epoxide amine reactions are 81.45 and 58.92 kJ mol^{-1}, respectively, while that for the etherification reaction is significantly higher, at 154.12 kJ mol^{-1}.

With this model it is possible to perform calculations in order to acquire a better understanding of how the system behaves under different circumstances. Figure 10 shows the predicted curve for $d\alpha/dt$ as a function of α for each curing temperature. The curve is decomposed to show the contributions from the three different reactions involved, i.e. A_1–*E*, A_2–*E* and OH–*E*. For α=0–0.2, the OH–*E* contribution is negligible. For α between 0.2 and 0.8, all three reactions are significant. For α between 0.2 and 0.6, the epoxide amine reactions are more important than the OH–*E* reaction. At α=0.6, the A_1–*E* reaction becomes negligible and the OH–*E* reaction becomes the most important. Finally, at α around 0.8, the A_2–*E* reaction becomes negligible.

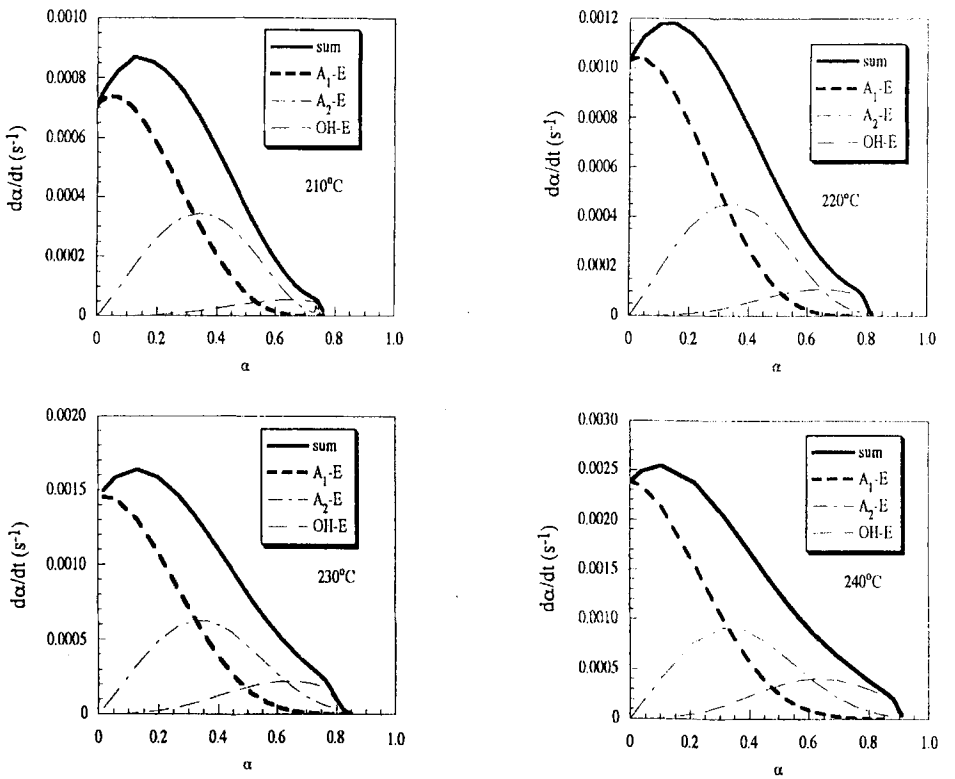

Fig. 10 Calculated curves for $d\alpha/dt$ as a function of α at different curing temperatures, showing the separate contributions from the A_1–*E*, A_2–*E* and OH–*E* reactions

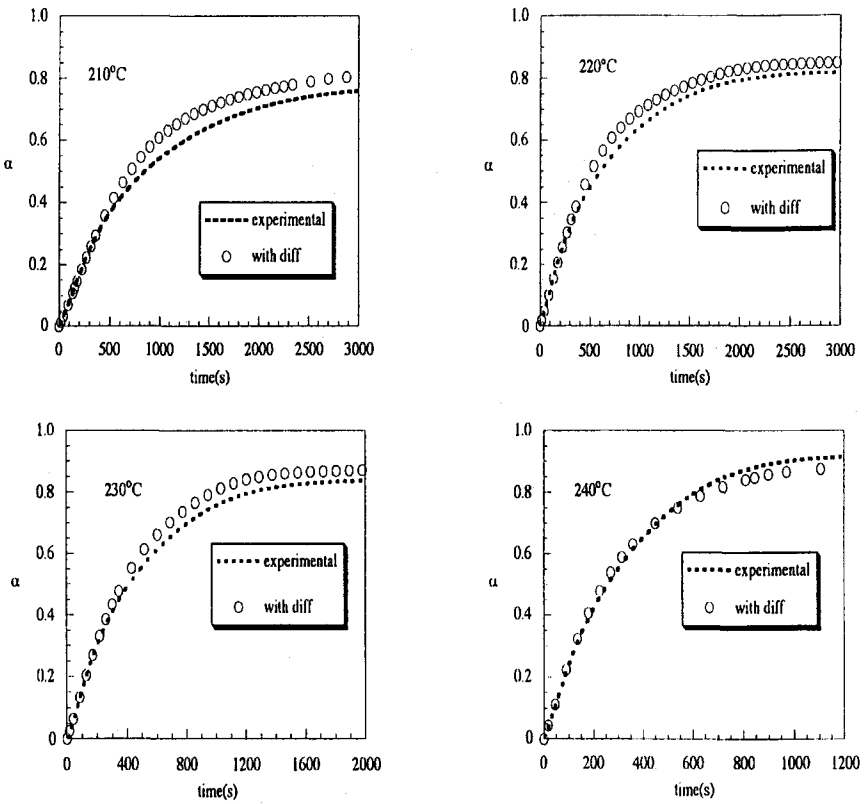

Fig. 11 Evolution of α with time for each curing temperature

Figures 5 and 9 reveal deviations between the experimental data and the model proposed for α between 0.2 and 0.5. Figure 10 demonstrates that, in this interval, the predominant reactions are the epoxide amine reactions. The model assumes equal relative reactivities for the primary amine groups initially present and the secondary amine groups formed in the reaction. The deviations observed could be attributed to different relative reactivities of the secondary and primary amine groups, but this is a question that has not been satisfactorily answered and will only be resolved by further experimental work.

It is also possible to predict the evolution of the cure with time. Figure 11 shows this evolution for each curing temperature, the experimental data being compared with the behavior predicted by the model with the diffusion factor included. Furthermore, the concentrations of the different species can be calculated from this model. Figure 12 and 13 depict the predicted concentrations of the different species as a function of time for each curing temperature with respect to the initial concentrations of epoxide groups, E_o. In all cases, it can be noted that at around α=0.45 over 90% of the A_1 groups have disappeared, but

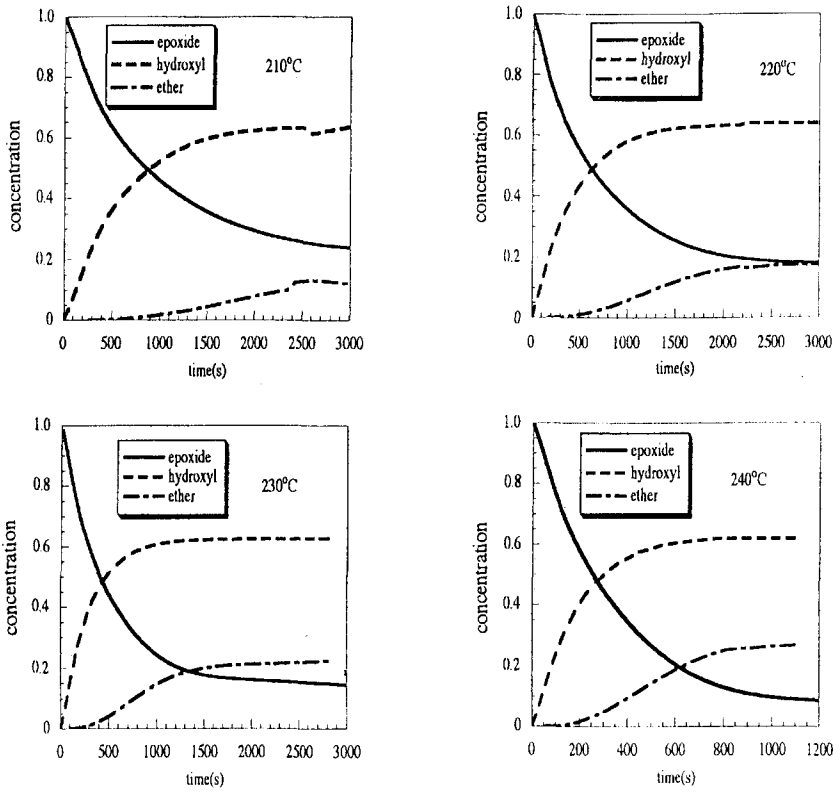

Fig. 12 Calculated concentrations of epoxide, hydroxy and ether groups as a function of time for each curing temperature

ether formation is just starting to become important. However, the A_2–E reaction, which produces A_3 groups, is significant both before and after α=0.45. Analysis of these last Figures demonstrates that at 210°C the critical value for diffusion control, α_c=0.75, is reached after 1900 s. At this point, 65% of the epoxide groups have reacted with amine, 10% have reacted with OH, and 25% remain unreacted. A similar analysis was made at each curing temperature, and the resume is shown in Table 2.

Table 2 Breakdown of epoxide group reaction

T/°C	α_c	t/s	E–A	E–OH	Unreacted
			%		
210	0.75	1900	65	10	25
220	0.80	1650	65	13	22
230	0.80	1000	62	14	24
240	0.90	850	62	25	13

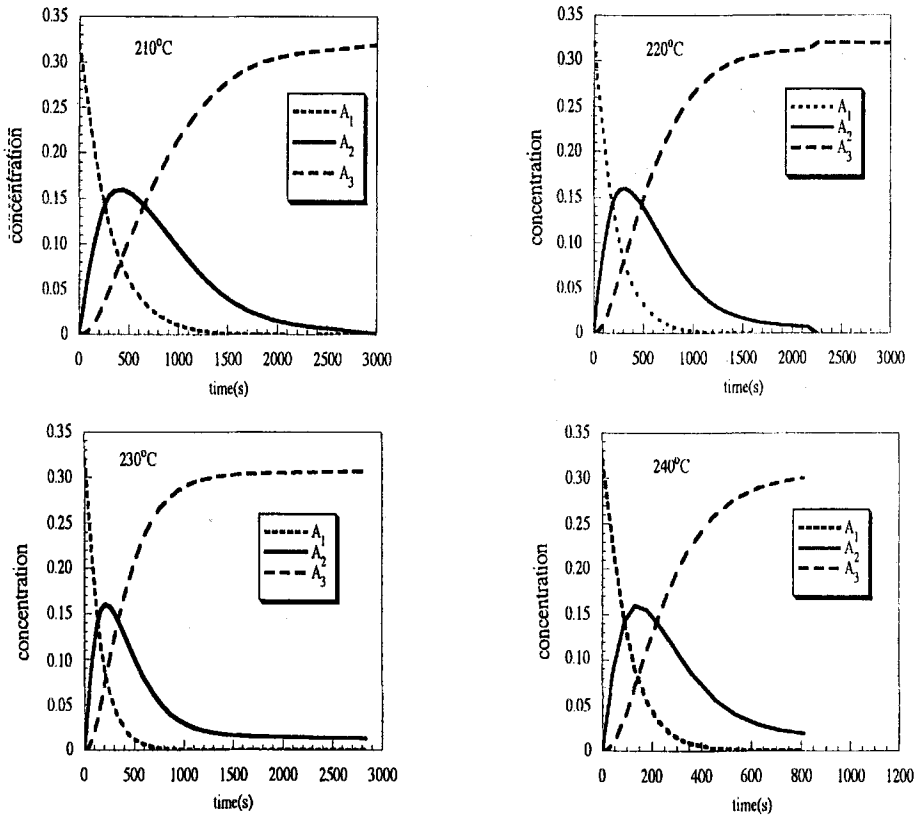

Fig. 13 Calculated concentrations of primary amine (A_1), secondary amine (A_2) and tertiary amine (A_3) groups for each curing temperature

Thus, at the point where vitrification slows down the reaction significantly, the epoxide amine reaction is virtually complete, regardless of temperature, but the epoxide OH reaction is only partially complete. At higher temperatures, more ether linkages are formed, as expected.

In subsequent work in our laboratory [20], we have studied the conditions of temperature and curing time for gelation and vitrification to appear, and the representation of such conditions in an isothermal time-temperature-transformation (*TTT*) diagram for this system. The maximum glass transition temperature determined for this epoxy was 242°C.

Conclusions

A mechanistic model proposed by Cole was employed to describe the kinetics of polymerization of a TGDDM/Novolac/DDS epoxy resin system. This

model is based on the Horie model, but is extended to include the etherification reaction.

The kinetics was described in terms of three rate constants, which were determined to fit the data. The rate constants obey the Arrhenius relationship. Values of the activation energies were determined. The kinetics was assumed to be of first order with respect to all participating species. The model gives a reasonable fit to the experimental data for values of α up to the critical point where the resin vitrifies and the reaction becomes diffusion-controlled. To describe the cure in this region, a diffusion factor was introduced, the model then allowing a prediction of the cure kinetics over the whole range of conversion, including the evolution of the different chemical species during the curing process.

* * *

This work was supported by the Xunta de Galicia through grant XUGA-17201A95. The authors wish to thank Ciba-Geigy for supplying the MY 720 and EPN 1138 prepolymers.

References

1 J. Mijovic, J. Kim and J. Slaby, J. Appl. Polym. Sci., 29 (1984) 1449.
2 J. M. Barton, Br. Polym. J., 18 (1986) 37.
3 R. J. Morgan and E. T. Mones, J. Appl. Polym. Sci., 33 (1987) 999.
4 L. Chiao, Macromolecules, 23 (1990) 1286.
5 J. D. Keenan, J. C. Seferis and J. T. Quinlivan, J. Appl. Polym. Sci., 24 (1979) 2375.
6 E. B. Stark, A. M. Ibrahim and J. C. Seferis, Interrelations between Processing Structure and Properties of Polymeric Materials, J. C. Seferis and P. S. Theocaris (eds), Elsevier, Amsterdam 1984.
7 K. C. Cole, J. J. Hechler and D. Noel, Macromolecules., 24 (1991) 3098.
8 K. C. Cole, Macromolecules, 24 (1991) 3093.
9 L. Matejka and K. Dusek, Macromolecules, 22 (1989) 2902.
10 J. Mijovic, A. Fishbain and J. Wijana, Macromolecules, 25 (1992) 979.
11 J. Mijovic and J. Wijana, Polym. Commun, 35 (1994) 2683.
12 J. M. Barton, Adv. Polym. Sci., 72 (1985) 111.
13 K. Horie, H. Hiura, M. Sawada, L. Mita and H. Kambe, J. Polym. Sci. Part A–1, 8 (1970) 1357.
14 H. Jahn and P. Goetzky, Epoxy Resins. Chemistry and Technology. 2nd ed, C. A. May Ed, Marcel Dekker, 1988. Chap 13.
15 W. I. Lee, A. C. Loos and G. S. Springer, J. Compos. Mater. 16 (1982) 510.
16 C. S. Chern and G. W. Poehlein, Polym. Eng. Sci., 27 (1987) 782.
17 S. E. Rabinowitch, Trans Faraday Soc., 33 (1937) 1225.
18 U. Khanna and M. Chanda, J. Appl. Polym. Sci., 49 (1993) 319.
19 L. Barral, J. Cano, A. J. López, J. López, P. Nogueira and C. Ramírez, J. Appl. Polym. Sci., 56 (1995) 1029.
20 L. Barral, J. Cano, J. López, P. Nogueira, C. Ramírez and M. J. Abad, Polym. Int., 42 (1997) 301.